

# Quantifying Biases in Non-Steady-State Chamber Measurements of Soil–Atmosphere Gas Exchange

Rodney T. Venterea<sup>1</sup>, Timothy B. Parkin<sup>2</sup>

<sup>1</sup>U.S. Department of Agriculture, Agricultural Research Service, Soil and Water Management Research Unit, St. Paul, MN

<sup>2</sup>U.S. Department of Agriculture, Agricultural Research Service, National Laboratory for Agriculture and the Environment, Ames, IA

327

## CHAPTER OUTLINE

Introduction 327

Physical Basis for the Chamber  
Effect 328

Experimental Approaches 330

Non-Linear Flux Calculation  
Schemes 330

Bias Estimation Techniques 331

Soil Property Effects 332

Chamber Bias Correction (CBC) 334

Limitations of the CBC Method 337

Bias Versus Precision 337

Current Recommendations 337

Ultimate Solutions 339

Appendix: Steps and Calculations Used in  
CBC Method 341

**Abbreviations:** CBC, chamber bias correction; CEAT, chamber error assessment tool; DP, deployment period; *F*, flux; GHG, greenhouse gas; *H*, height or volume-to-area ratio; HM, Hutchinson and Mosier (1981); HMR, revised Hutchinson and Mosier (1981); LR, linear regression; NDFF, non-linear diffusive flux estimator; NSS, non-steady state; PDF, pre-deployment flux; *TFU*, theoretical flux underestimation

## INTRODUCTION

Chamber techniques offer the best currently available tool for statistically evaluating the effects of management practices and potential mitigation strategies on emissions of important trace and greenhouse gases (GHGs). However, limitations of non-steady-state (NSS) chamber methods for determining soil-to-atmosphere trace gas exchange rates have

been recognized for several decades (Hutchinson and Mosier, 1981). Of these limitations, the so-called “chamber effect” is one of the most challenging to overcome. The chamber effect can be defined as the inherent tendency for NSS gas flux chamber methods to produce a biased estimate of the actual pre-deployment flux (PDF), where the PDF is defined as the flux occurring immediately prior to placement of the chamber on the soil surface (Mathias et al., 1978; Healy et al., 1996; Livingston et al., 2006; Kutzbach et al., 2007; Kroon et al., 2008; Pederson et al., 2010). This effect can be particularly important for GHGs like nitrous oxide ( $\text{N}_2\text{O}$ ) which often require more prolonged chamber deployment periods in order to facilitate analytical measurement. Despite widespread recognition of this limitation, there is little consensus regarding practical approaches to either estimating or reducing the magnitude of this effect. Rochette and Eriksen-Hamel (2008) showed that there is wide variation in method protocols used to determine soil  $\text{N}_2\text{O}$  flux, details of which can directly affect chamber-induced bias. Recent analysis has shown that intra- and inter-site flux comparisons can be confounded by chamber-induced artifacts (Venterea, 2010). Since NSS chambers generally tend to underestimate the actual PDF, this raises the likelihood that current emissions assessments at the regional, national, and global scale are negatively biased. This has important implications for effective management and mitigation of GHG emissions. The main objectives of this chapter are to (1) describe the physical basis of the chamber effect and how measurement methods and soil properties influence this effect, (2) describe currently available options for quantifying and minimizing flux estimation errors, and (3) briefly discuss the path toward solutions to this problem.

## PHYSICAL BASIS FOR THE CHAMBER EFFECT

Most if not all researchers using NSS chambers are well aware of the general problem posed by the chamber effect. Its fundamental basis is that gas exchange between soil and the atmosphere is driven in most circumstances by diffusion (Hutchinson and Livingston, 2002). We know from Fick’s law that the diffusive flux ( $F$ , with units<sup>a</sup> of  $\text{M L}^{-2} \text{soil T}^{-1}$ ) is proportional to the concentration gradient ( $dC/dz$ ) at the soil–atmosphere interface, where the gradient is defined as the derivative of the gas concentration ( $C$ ,  $\text{M L}^{-3}$  gas) in the direction of the flux, or, under steady-state conditions

$$F = D_s \frac{dC}{dz} \quad [1]$$

where  $z$  indicates vertical distance ( $L$ ) and  $D_s$  ( $L^2 \text{ gas L}^{-1} \text{ soil T}^{-1}$ ) is the soil gas diffusivity. NSS chamber methods rely on placement of an enclosure on the soil surface, within which gases generated in the soil are allowed to accumulate for a given deployment period (DP). This accumulation of gas within the chamber alters the concentration gradient at the soil–atmosphere interface and therefore the soil–atmosphere flux. Thus, we are confronted with the situation where attempting to measure a quantity immediately alters its magnitude, which is a classical problem for other physical measurements such as temperature (Griffiths, 1926). Following chamber deployment, gas concentrations will not only change within the chamber itself, but also within the air-filled pores of the soil beneath the chamber. Depending on the insertion depth of the chamber walls into the soil, this may create horizontal gradients in trace gas concentrations in soil directly under and immediately adjacent to the chamber. This may induce lateral trace gas diffusion within the soil. This effect, as well as leakage of gas to the outside atmosphere from an improperly sealed chamber, may also alter chamber gas concentration dynamics and cause negatively biased estimates (Pedersen et al., 2010).

<sup>a</sup> Unit dimensions are indicated by  $M$  for mass,  $L$  for length, and  $T$  for time. Where appropriate, dimensions are also specified with respect to the quantity described by the unit, i.e. soil, gas,  $\text{H}_2\text{O}$ .

While the soil-to-atmosphere flux depends directly on the concentration gradient, which is a spatial derivative (i.e.  $(dC/dz)$  in Eq. [1]), in practice the flux using NSS chambers is calculated based on estimation of a time derivative. That is, flux is determined from the change in trace gas concentration over time in samples of the chamber contents taken at multiple times during the DP. In the simplest case,  $F$  can be estimated from

$$F = \frac{dC}{dt} \frac{V}{A} \quad [2]$$

where  $dC/dt$  is the linear regression (LR)-based slope of the chamber gas concentration versus time ( $t$ ),  $V$  is the internal chamber volume ( $L^3$  gas), and  $A$  is the soil surface area ( $L^2$  soil) enclosed by the chamber. It is also convenient to define the chamber height ( $H$ ) as the ratio of  $V$  to  $A$ , having units of  $L^3$  gas  $L^{-2}$  soil which are commonly simplified to units of  $L$  (e.g. cm).

In cases where the direction of gas flux is from soil to atmosphere, which is usually considered to be a flux in the “positive” direction, gas concentration will increase in the chamber over time. This will cause the vertical gradient at the soil–atmosphere interface,  $(dC/dz)$  in Eq. [1], and therefore the flux ( $F$ ) to decrease over time. This in turn will cause the time derivative,  $(dC/dt)$  in Eq. [2], obtained from measurements of chamber gas concentration, to decrease with time leading to the type of curvature shown in Figure 19.1 for a positive flux. Conversely, in cases where the flux is from atmosphere to soil (i.e. a “negative” initial flux), gas concentration will decrease in the chamber with time, thereby causing  $(dC/dz)$  at the soil–atmosphere interface and  $F$  to increase (i.e. become less negative) over time. This in turn causes  $(dC/dt)$  in Eq. [2] to increase with time, leading to the type of curvature shown in Figure 19.1 for a negative flux.

The remainder of this chapter will focus on the case of positive flux, which is generally found for carbon dioxide ( $\text{CO}_2$ ) and  $\text{N}_2\text{O}$ . The approaches to be discussed here are not expected to apply to negative fluxes, which are commonly observed for gases including methane and nitric oxide. Such negative fluxes are influenced by biologically mediated gas consumption within the soil. Emissions of  $\text{N}_2\text{O}$  can also be influenced by biological transformation, i.e. denitrification. Using process-based modeling, Venterea et al. (2009) showed that biological consumption of  $\text{N}_2\text{O}$  in the soil profile is not likely to affect chamber  $\text{N}_2\text{O}$  concentration dynamics, except under extreme conditions. However, the significance of negative  $\text{N}_2\text{O}$  fluxes is currently a topic of research (Chapuis-Lardy et al., 2007). Senevirathna et al. (2007) developed a detailed numerical model that may provide some guidance for addressing the influence of biological consumption on chamber dynamics and flux calculations.

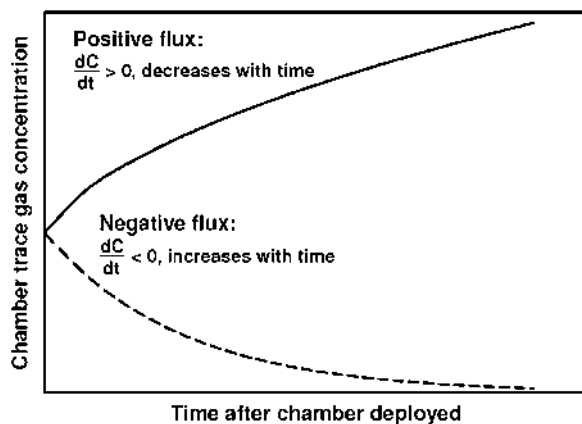


**FIGURE 19.1**

Hypothetical, generalized shapes of chamber time series data as affected by alteration of the concentration gradient at the soil–atmosphere interface for the case of positive and negative fluxes.

It is logical to expect that the degree of bias in a flux estimate based on Eq. [1] will increase when longer DPs are used, since  $dC/dt$  will be expected to change to a greater degree as time increases (Figure 19.1). Also, for a given DP, a smaller value of  $H$  would be expected to result in a greater increase in chamber concentration for a given flux, due to less dilution by the air initially present in the smaller chamber. Thus, it is also logical to expect that the degree of bias in a flux estimate will increase as  $H$  decreases. While these two general guidelines (i.e. bias increases with longer DP and smaller  $H$ ) can be deduced based on a qualitative understanding of the chamber effect, they do not provide any quantitative information or practical guidance regarding the magnitude of the bias associated with any particular set of deployment conditions. They also do not indicate which set of measurement conditions will provide a reasonable or acceptable degree of bias.

## EXPERIMENTAL APPROACHES

Experimental approaches have been used to attempt to directly measure the degree of chamber-induced bias. The main challenge of an experimental approach is that, at least under field conditions, it is generally impossible to have knowledge of the actual PDF, since any attempt to measure it will necessarily modify it. Thus, laboratory investigations have attempted to utilize various experimental systems designed to create a flux of known magnitude through a porous medium (Ney et al., 1994; Pumpanen et al., 2004; Widen and Lindroth, 2003; Butnor and Johnsen, 2004; Martin et al., 2004; Butnor et al., 2005). Limitations of this approach have been two-fold: (1) it is problematic to create an experimental system which maintains a known and steady flux for sufficient duration while also maintaining diffusion as the dominant transport process (i.e. minimizing pressure gradients); and (2) any relationships obtained between the measured flux and the PDF will likely be limited in applicability to the particular set of measurement conditions evaluated (i.e. DP,  $H$ , and media properties).

## NON-LINEAR FLUX CALCULATION SCHEMES

Due to the limitations described above with regard to experimental methods, theoretical and numerical approaches have been used to develop bias correction techniques. Currently, the most commonly used approach for bias correction is to apply a flux calculation (FC) scheme that estimates the PDF by fitting a non-linear function to the chamber time series data. The available non-linear FC schemes include what we will refer to as (1) Type I, or entirely empirical approaches, which include polynomial functions which are not derived from any particular theoretical considerations, e.g. the quadratic model of Wagner et al. (1997); (2) Type II, or semi-theoretical approaches based on relatively simplified gas transport theory, in particular the model of Hutchinson and Mosier (1981) (HM), and a revised version of the HM model (HMR) of Pedersen et al. (2010); and (3) Type III, or theoretical approaches that are based on more rigorous gas transport theory, e.g. Livingston et al. (2006) and Venterea (2010). Type I and II schemes use various means to estimate the value of  $(dC/dt)$  at the moment of chamber deployment ( $t = 0$ ), and then use this estimate in Eq. [1] to calculate  $F$ , while Type III methods do not calculate  $(dC/dt)$  directly, but utilize different numerical approaches to estimate the PDF.

Prior to the study by Livingston et al. (2006), it was widely assumed that Type I and II FC schemes provided reasonably effective correction of chamber-induced bias. The major advance of Livingston et al. (2006) was derivation of an analytical solution to a soil-gas transport equation describing one-dimensional (1D) diffusive flux of a trace gas from the soil into a closed chamber, assuming certain physical conditions (described below). Under these conditions, Livingston et al. (2006) clearly showed that previously developed Type I and II FC schemes do not fully account for chamber-induced biases.

Livingston et al. (2006) also presented a new (Type III) FC scheme called the non-linear diffusive flux estimator (or NDFE, software available at <http://arsagsoftware.ars.usda.gov>)

which, as mentioned above, is based on soil-gas transport theory with the following assumptions: (1) flux is driven by diffusion; i.e. pressure gradients are minimal, (2) diffusive flux is primarily 1D in the vertical direction; i.e. horizontal transport is minimal, (3) the chamber atmosphere is homogeneously mixed, (4) leakage out of the chamber is negligible, (5) irreversible consumption of gas in the soil (e.g. biological uptake) or in the chamber (e.g. gas-phase or surface reaction) is negligible, and (6) soil physical properties (i.e. total and air-filled porosity) are vertically uniform. Livingston et al. (2006) concluded that with a properly designed chamber, i.e. having appropriately sized vent tube and chamber insertion depth (Hutchinson and Livingston, 2002), assumptions (1) through (4) are generally valid, and therefore that the NDFE scheme is superior to all others. As mentioned above, assumption (5) appears to be generally valid for CO<sub>2</sub> and N<sub>2</sub>O.

However, even when the above assumptions are valid, the NDFE scheme is relatively inefficient to apply to large datasets. The method requires non-linear iterative regression, will often arrive at multiple solutions for a given data set (Venterea and Baker, 2008), and can deliver flux estimates that are much greater than expected (Pedersen et al., 2010). Due to these issues, the NDFE model has seen limited application. Also, the general validity of some of the underlying assumptions have been questioned by Venterea and Baker (2008) (assumption 6) and Pedersen et al. (2010) (assumption 2). In spite of these limitations, the work of Livingston et al. (2006) has turned out to be useful in developing methods that provide at least an approximate estimate of the degree of chamber-induced bias.

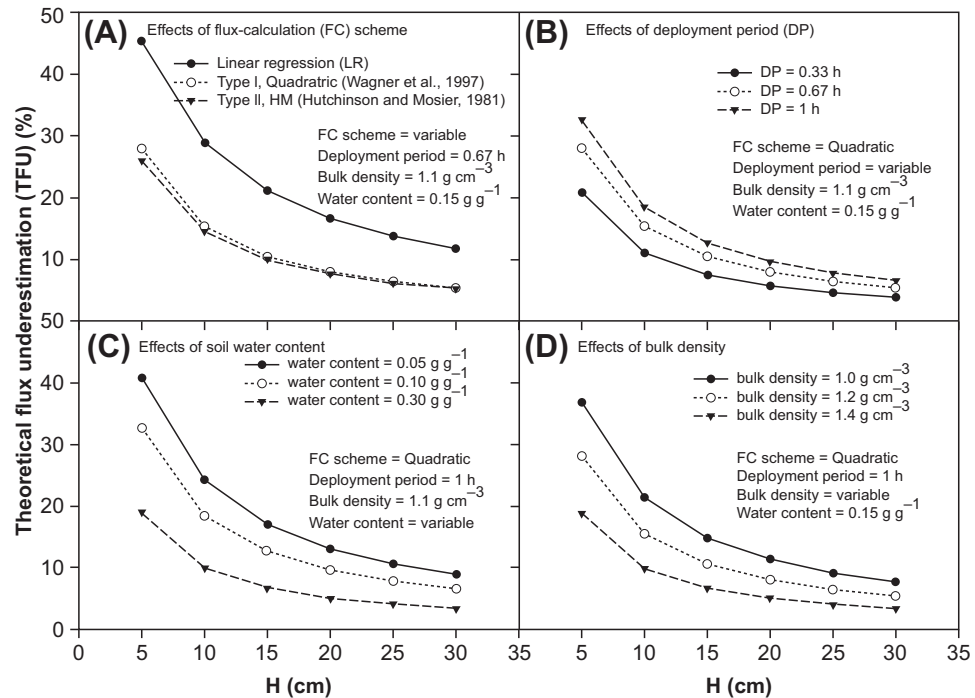
## BIAS ESTIMATION TECHNIQUES

Venterea et al. (2009) utilized the analytical solution of Livingston et al. (2006) to develop a spreadsheet-based Chamber Error Assessment Tool (CEAT) to estimate the degree of chamber-induced bias which may be useful in designing chambers and selecting DPs. The CEAT spreadsheet is available online at <http://www.ars.usda.gov/pandp/docs.htm?docid=18991> or upon request from the authors. Given basic information regarding  $H$ , DP, and soil properties, CEAT generates theoretical chamber concentration time series data as well as the theoretical flux underestimation ( $TFU$ , %) of the PDE, where

$$TFU = 100 \frac{(PDF - F)}{PDF} \quad [3]$$

The  $TFU$  is one way to express the bias of the flux estimate. By this definition, a positive value of  $TFU$  indicates that the  $F$  has been *underestimated*. For each set of conditions, CEAT estimates  $TFU$  for  $F$  calculated using LR as well as using Type I (quadratic) and Type II (HM) non-linear FC schemes.

It is important to note two critical findings of Livingston et al. (2006), i.e. the  $TFU$  calculated using Eq. [3] is independent of: (1) the PDE, and (2) the vertical distribution of trace gas production in the soil. Both of these findings may be counterintuitive, since it might be expected that, following chamber deployment, (1) a greater PDF would lead to greater and more rapid suppression of the inter-facial concentration gradient, and (2) trace gas production that is located closer to the soil surface may result in more deformation of the soil-atmosphere concentration gradient after chamber placement. For (1), since  $TFU$  is calculated relative to the PDE, it turns out that  $TFU$  is independent of the PDE. Finding (2) is more difficult to explain without a mathematical presentation, but was confirmed by Venterea and Baker (2008) using numerical modeling methods under a range of assumed production profiles. Findings (1) and (2) above greatly simplify bias estimation techniques. The result is that when  $TFU$  is calculated as a function of  $H$ , DP, and soil physical properties, the result can be generalized to varying flux magnitudes independent of the vertical distribution of gas production within the soil profile. Examples of CEAT output are given in Figure 19.2. These results illustrate that Type I and II non-linear schemes do not completely eliminate

**FIGURE 19.2**

Theoretical flux underestimation (*TFU*) determined using the Chamber Error Assessment Tool (CEAT) as a function of the chamber volume to area ratio (*H*) and varying (A) flux calculation (FC) schemes, (B) deployment periods (DP), (C) gravimetric water content, and (D) bulk density.

chamber-induced biases. They also show how *TFU* increases with decreasing *H*, increasing DP, and differences in soil properties.

## SOIL PROPERTY EFFECTS

As illustrated in Figure 19.2, soil physical properties will influence the magnitude of diffusion-driven, chamber-induced bias. These effects have been noted by Hutchinson et al. (2000), Venterea and Baker (2008) and Venterea et al. (2009). Gas transport theory predicts that increased soil air-filled porosity ( $\epsilon$ ) leads to increased non-linearity in chamber time series data, which results in increased *TFU*. Thus, if we compare soil profiles that differ with respect to  $\epsilon$  but have the same PDF, the profile with greater  $\epsilon$  will be expected to result in chamber time series data with more curvature and therefore a greater magnitude of bias (i.e. a greater *TFU*).

This effect can be illustrated with the CEAT spreadsheet tool which can be used to generate simulated chamber time series for different soil profiles assumed to have the same PDF but different physical properties. For example, in Figure 19.3, hypothetical soil profiles 1 and 2 are both assumed to have a PDF of  $100 \mu\text{g N m}^{-2} \text{h}^{-1}$  and the same gravimetric water content ( $0.15 \text{ g g}^{-1}$ ), but with bulk densities of  $1.0$  and  $1.4 \text{ g cm}^{-3}$ , respectively, resulting in  $\epsilon$  values of  $0.47$  and  $0.26 \text{ cm}^3 \text{ cm}^{-3}$ , respectively. Comparing the chamber time series data for profiles 1 and 2 with  $H = 5 \text{ cm}$  (Figure 19.3, upper curves), profile 1 (with greater  $\epsilon$ ) displays more non-linearity in the data and thus will lead to greater flux underestimation than profile 2. The CEAT-calculated *TFUs* for these same conditions for DP = 1 h are illustrated in Figure 19.2D. This effect diminishes with increased *H* and decreased DP. Thus, the chamber time series for profiles 1 and 2 tend to converge for  $H = 30 \text{ cm}$  and DP < 0.5 (Figure 19.3, lower curves).

Since the effect of soil physical properties on chamber dynamics is not widely recognized, it is worth exploring its physical basis and practical implications. Fundamentally, what is

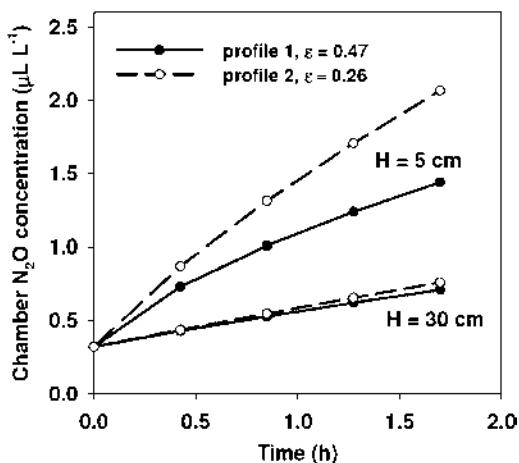


**FIGURE 19.3**

Theoretical chamber time series data generated using the Chamber Error Assessment Tool (CEAT) for two uniform soil profiles (1 and 2) assuming the same pre-deployment flux ( $100 \mu\text{g N}_2\text{O-N m}^{-2} \text{h}^{-1}$ ) and varying chamber volume to area ratios ( $H$ ). Profiles 1 and 2 were assumed to have the same gravimetric water content ( $0.15 \text{ g H}_2\text{O g}^{-1}$ ) but varying bulk density ( $1.0$  and  $1.4 \text{ g cm}^{-3}$ , respectively), resulting in varying air-filled porosity ( $\epsilon$ ).

happening is that following chamber deployment, the soil with greater  $\epsilon$  will accumulate more trace gas in the soil pores, therefore allowing less gas to diffuse into the chamber, compared to the soil with lower  $\epsilon$ . This effect can be illustrated by dynamic modeling of soil-gas concentration profiles below the chamber following deployment using numerical techniques (e.g. Venterea and Baker, 2008). First of all, the soil with greater  $\epsilon$  (in the above example, profile 1) will also have greater soil-gas diffusivity ( $D_s$ ), since  $D_s$  increases with increasing  $\epsilon$  (Rolston and Moldrup, 2002). Therefore, prior to chamber deployment, according to Fick's law (Eq. [1]), the soil with greater  $\epsilon$  and  $D_s$  will have a proportionally smaller gradient ( $dC/dz$ ) for a given PDF compared to the soil with smaller  $\epsilon$ . This results in different initial concentration gradients for profiles 1 and 2, as illustrated in Figure 19.4 for  $t = 0$  h.

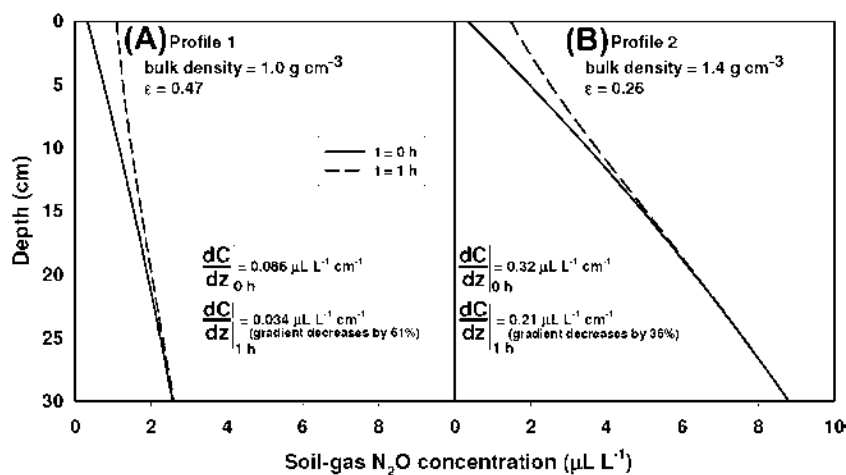


**FIGURE 19.4**

$\text{N}_2\text{O}$  soil-gas concentration profiles prior to ( $t = 0$  h) and after ( $t = 1$  h) chamber deployment for (A) profile 1 and (B) profile 2, assuming pre-deployment flux of  $100 \mu\text{g N}_2\text{O-N m}^{-2} \text{h}^{-1}$  and chamber volume to area ratio ( $H$ ) of 5 cm. Values of the vertical gradient at the soil-atmosphere interface ( $dC/dz$ ) were calculated from the linear regression slope over the 0 to 5 cm depth. Data were generated using the model of Venterea and Baker (2008).

When the chamber is deployed, gas accumulates at the soil surface (i.e. in the chamber) causing the soil–atmosphere concentration gradients ( $dC/dz$ ) in both soils to be deformed (decreased) from their original pre-deployment state. Diffusion theory predicts that the initially smaller gradient present in the less dense, high- $\epsilon$  soil will be deformed to a greater extent (profile 1, decreased by 61%) compared to the gradient in the more dense, low- $\epsilon$  soil (profile 2, decreased by only 21%), as illustrated in Figure 19.4 for  $t = 1$  h. Due both to the greater degree of deformation and the greater  $\epsilon$  of the less dense soil (profile 1), the net result is that more gas accumulates within the soil pores of profile 1 compared with profile 2 over a given period of time. Because gas is produced at the same rate in both soils, since they have the same PDF, this means that less gas is available to diffuse into the chamber above profile 1. For the current example, the model calculates that 57% of the  $N_2O$  produced in the soil over a 1 h period following chamber deployment accumulates within the soil for profile 1, allowing only 43% of the  $N_2O$  produced to diffuse into the chamber. In contrast, 37% of the  $N_2O$  produced in the soil accumulates within the soil for profile 2, and 63% diffuses into the chamber. These differences in soil-gas storage and diffusion rates lead to the differences in chamber gas concentration data shown in Figure 19.3.

The effect described above can lead to two potentially important experimental artifacts. First, it can confound the comparison of fluxes measured within the same soil profile at different times due to varying water content. That is, since drier conditions will result in greater  $\epsilon$ , assuming a relatively constant bulk density over time, greater non-linearity in chamber data and greater potential for underestimating the actual PDF will be expected under drier conditions. As described by Venterea (2010), this effect could lead to an apparent positive correlation between soil water content and gas flux within the same soil, when in fact the observation is an artifact of chamber-induced bias. Second, the soil property effect can confound the comparison of fluxes among soils having different physical properties resulting from either natural variation or experimental manipulation, for example when gas fluxes are compared among soils treated with different tillage or water management regimes (e.g. Omonode et al., 2011), or soils amended with different types or amounts of organic materials (e.g. Rochette et al., 2008). In this case, chamber-induced biases could lead to the mistaken conclusion that soils with greater bulk-density have greater gas fluxes. For the current example illustrated in Figures 19.3–19.4, assuming  $H = 5$  cm and  $DP = 1$  h, applying the quadratic FC scheme of Wagner et al. (1997) to the chamber data for profile 1 would generate a flux estimate of  $63 \mu\text{g N m}^{-2} \text{h}^{-1}$  compared with  $81 \mu\text{g N m}^{-2} \text{h}^{-1}$  for profile 2. Thus, the less dense soil appears to have a flux that is 22% less than the more dense soil, while in reality their fluxes are the same. The magnitude of this effect will be influenced by chamber geometry and deployment time. For example, for chamber data using  $H = 30$  cm and  $DP = 1$  h, the quadratic FC scheme estimates fluxes of 92 and  $97 \mu\text{g N m}^{-2} \text{h}^{-1}$  for profiles 1 and 2, respectively, a difference of only 5%.

### CHAMBER BIAS CORRECTION (CBC)

The artifacts of soil property effects described above will be most pronounced when LR is used; however, the artifacts do not disappear when Type I or II non-linear FC schemes are used. In theory, the NDFE scheme eliminates these artifacts for a completely uniform soil profile. However, practical and theoretical limitations of the NDFE scheme (described above) are problematic. Venterea (2010) developed a chamber bias correction (CBC) technique that overcomes some of the limitations of the NDFE method. The CBC method is based on the same theory as Livingston et al. (2006), but is readily adapted to spreadsheets, delivers a single result, and reduces the frequency of suspiciously large flux estimates. An outline of the CBC method is given below, and full details for its application are provided in the Appendix. The CBC method can be used in one of two ways: (1) a graphical option that can be used for approximating the degree of bias associated with a particular chamber method applied to a particular soil, similar to CEAT; or (2) a fully numerical option can be used for making



**TABLE 19.1** Input Parameters Required for Applying the Chamber Bias Correction (CBC) Method, and Parameter Values for Example Soil Profiles

Parameter	Symbol	Units	Example profiles		
			1	2	3 <sup>‡</sup>
Bulk density	$\rho$	g dry soil cm <sup>-3</sup> bulk soil	1.0	1.4	1.19
Particle density	$\rho_p$	g dry soil cm <sup>-3</sup> soil particle	2.65	2.65	2.65
Water content	$\theta$	cm <sup>3</sup> H <sub>2</sub> O cm <sup>-3</sup> soil	0.15	0.21	0.14
Soil temperature	$T_s$	°C	20	20	20
Clay fraction	CF	g clay g <sup>-1</sup> soil	0.22	0.22	0.22
Soil pH <sup>†</sup>	pH	—	na	na	na
Volume-to-area ratio	H	cm <sup>3</sup> gas cm <sup>-2</sup> soil	5	5	10
Deployment period	DP	h	1.0	1.0	0.85, 1.7 <sup>§</sup>

<sup>†</sup>Soil pH is needed for CO<sub>2</sub> only (see Appendix).

<sup>‡</sup>Profile 3 has non-uniform soil properties (see Figure 19.5). Bulk density and water content values in the table are for samples taken from 0–10 cm depth interval.

<sup>§</sup>Two different values of DP (0.85 and 1.7 h) are examined for profile 3.

quantitative bias corrections. In the latter case, since many of the required properties (Table 19.1) will vary over time, the most accurate results will be obtained if the properties are measured with an appropriate degree of temporal resolution to capture this variation. Additionally, some of these properties (e.g. bulk density, water content, temperature) also tend to vary with depth. This issue of vertical non-uniformity in soil properties is addressed in the examples given below.

There are three general steps involved in applying the CBC method for both the graphical and numerical options:

1. The initial flux estimate ( $F$ ) is calculated in the conventional manner using either LR, the Type I quadratic method (Wagner et al., 1997), or the Type II HM method (Hutchinson and Mosier, 1981).
2. The degree of bias associated with the initial flux estimate is determined and expressed as  $TFU$  (% basis)
3. The PDF is determined by rearranging Eq. [3] and solving for PDF knowing  $F$  and  $TFU$ .

Step 2 (determining  $TFU$ ) consists of calculating values of two scaling parameters  $E_1$  and  $E_2$ , which are then used together to calculate  $TFU$ . The parameter  $E_1$  accounts for soil property effects, while the parameter  $E_2$  accounts for the effects of  $H$  and  $DP$ . The difference between the more approximate graphical option and the more rigorous numerical option is that with the graphical option the user determines  $E_1$  visually using nomograms (see Venterea, 2010), while the numerical option uses physically based calculations. While the numerical method for determining  $E_1$  is mathematically straightforward, it involves several calculation steps. These steps are presented in the Appendix, and a spreadsheet template containing the calculations is available for downloading at <http://www.ars.usda.gov/pandp/people/people.htm?personid=31831> or upon request from the authors. For the graphical technique, once  $E_1$  is obtained, the steps starting with Step 2c and Eq. [A8] in the Appendix can be followed.

As examples, the chamber time series data given in Figure 19.3 for the vertically uniform soil profiles (1 and 2) used for the previous example, as well as an additional, vertically non-uniform soil profile (profile 3), were analyzed using the CBC method. Profile 3 has vertically variable bulk density and water content (and therefore variable  $\epsilon$ ), as shown in Figure 19.5A, based on high-resolution measurements in a soil used for corn/soybean production under a moldboard plow tillage regime (Venterea and Baker, 2008). Chamber concentration time series data for profile 3 generated using the numerical model of

## SECTION 5

### Measurements and Monitoring

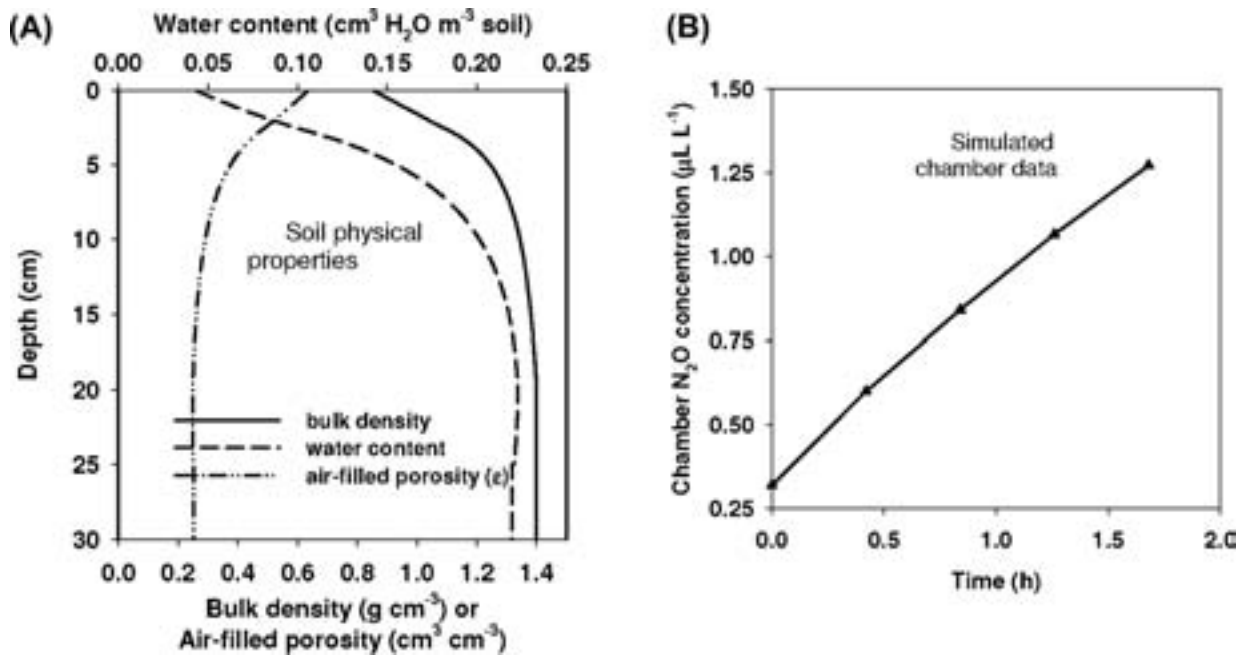


**FIGURE 19.5**

(A) Vertical profiles of bulk density, water content and air-filled porosity ( $\epsilon$ ) for profile 3; (B) chamber concentration data for profile 3 simulated using the model of Venterea and Baker (2008) assuming a pre-deployment flux (PDF) of  $100 \text{ g m}^{-2} \text{ h}^{-1}$  and chamber volume-to-area ratio ( $H$ ) of 10 cm. Lines in (A) were obtained by non-linear regression of measured bulk density and water content in a soil used for corn/soybean production under a moldboard plow tillage regime (Venterea and Baker, 2008).

336

Venterea and Baker (2008) are shown in Figure 19.5B, assuming a PDF of  $100 \mu\text{g N m}^{-2} \text{ h}^{-1}$  and  $H = 10 \text{ cm}$ .

Input parameter values required by the CBC method for each of the three profiles are given in Table 19.1. Obviously, for a non-uniform soil (e.g. profile 3), values of the required input parameters will depend on the sampling depth considered. Analysis of this and other non-uniform soil profiles has indicated that input parameters based on a 10 cm sampling depth will produce accurate *TFU*-correction (Venterea, 2011, unpublished data). Thus, bulk density and water content values that would be obtained for samples taken from 0–10 cm depth interval were used as input parameters for profile 3 (Table 19.1). Values of  $F$  estimated using the quadratic method of Wagner et al. (1997), and the calculated values of  $E_1$ ,  $E_2$ , *TFU* and PDF using the CBC method for all three soil profiles are given in Table 19.2. The estimated PDF values (last column of Table 19.2) are very close to the theoretical value ( $100 \mu\text{g N m}^{-2} \text{ h}^{-1}$ )

**TABLE 19.2** Values of the Uncorrected Flux ( $F$ ), the Two Scaling Parameters ( $E_1$  and  $E_2$ ) and the Calculated Pre-Deployment flux (PDF) for Three Different Soil Profiles and Measurement Conditions

Profile	H cm	DP h	$F^\dagger$ $\mu\text{g N m}^{-2}$ $\text{h}^{-1}$	$E_1^\ddagger$ $\text{cm}^6 \text{ gas cm}^{-4}$ $\text{soil h}^{-1}$	$E_2$ —	TFU %	Calculated PDF $\mu\text{g N m}^{-2} \text{ h}^{-1}$
1	5	1.0	63.0	53.7	-0.764	36.4	99.0
2	5	1.0	81.0	9.51	0.966	17.8	98.6
3	10	0.85	83.4	36.7	1.177	16.2	99.6
		1.7	77.9	36.7	0.4836	21.9	100.9

<sup>†</sup> $F$  values determined using the quadratic method of Wagner et al. (1997).

<sup>‡</sup>See Appendix for discussion about units for  $E_i$ .

that was used to generate the time series data. In contrast, the  $F$  values calculated using the quadratic method underestimated the PDF by 16 to 37% (Table 19.2).

## LIMITATIONS OF THE CBC METHOD

One limitation of the CBC method is that it requires values for soil properties listed in Table 19.1 as inputs. Thus, errors in estimation of these properties would necessarily lead to errors in the final flux estimates. Like measurement of any other variable soil property, these errors can be minimized by increasing the spatial and temporal intensity of sampling. Of course, this will increase the time and expense required for making flux estimates. To date, there has not been a sensitivity assessment of how errors in estimating these properties will translate into errors in flux estimation using the CBC method. This needs to be addressed in future studies.

Another potentially important limitation is the assumption of 1D vertical diffusion (assumption 2) within the theory underlying the CBC method. Livingston et al. (2006) concluded that the 1D assumption was reasonable in the case where chambers have wall-insertion depths that are properly sized with respect to soil physical properties. That is, soils expected to have greater  $\epsilon$  values should use chambers with deeper insertion depths. Guidelines put forth by Hutchinson and Livingston (2001, 2002) recommend wall depths of at least 5 cm, and as much as 20 cm, depending on soil properties and DPs. Pedersen et al. (2010) raised the possibility that, at least under certain conditions, the 1D assumption may not be reasonable. Pedersen et al. (2010) pointed out that the theory underlying the NDFE and CBC methods would predict chamber gas concentrations will continue to increase infinitely with extended DPs, but that this prediction is not consistent with empirical observation. Pedersen et al. (2010) also put forth a modification of the Hutchinson and Mosier (1981) FC scheme (the HMR model) which attempts to account for the possibility of both lateral (i.e. 2D) diffusion and leakage from an imperfectly sealed chamber (search HMR at <http://www.r-project.org/>). Future studies are required to evaluate the robustness of the HMR model.

## BIAS VERSUS PRECISION

This chapter has focused on *bias* estimation and correction, but another important consideration with regard to flux estimation errors is the *precision* of the method. While bias is the degree to which a flux estimate differs from the PDE, precision is the degree to which repeated estimates agree with each other (Figure 19.6). Practices that decrease the bias of flux estimates will also generally decrease the precision of those estimates (Venterea et al., 2009). Reducing the deployment period (DP), increasing the chamber height ( $H$ ), and utilizing non-linear FC schemes (relative to LR) all serve to reduce the bias of flux estimates. However, these same practices also reduce the precision of the flux estimates. The degree to which each of these practices will decrease the precision of the overall flux estimates will depend upon the precision of the sampling and analytical procedure used to determine the chamber headspace gas concentration. Nonlinear models such as the quadratic, HM and HMR methods are inherently more sensitive to small deviations in headspace concentration data. Thus, an inherent trade-off exists between the bias and precision of flux estimates obtained using a particular chamber configuration, deployment time, and FC scheme in a given soil (Venterea et al., 2009; Parkin and Venterea, 2010).

## CURRENT RECOMMENDATIONS

Gas transport theory predicts that variations in chamber methods and soil physical properties will affect not only the absolute magnitude of flux estimates, but also the relative difference in fluxes among soils that differ with regard to physical properties. This factor, together with the inherent trade-off between bias and precision described above, make it impossible to

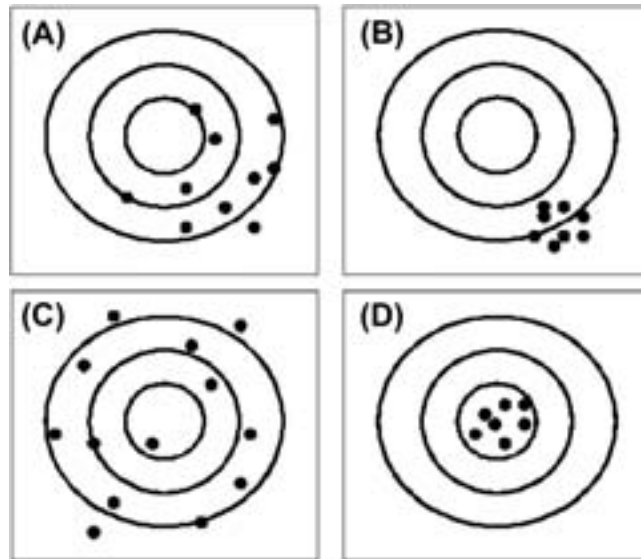
**FIGURE 19.6**

Diagram illustrating bias and precision of chamber methods. Bias is illustrated by how close the flux estimates (points) cluster around the target bull's-eye, which represents the pre-deployment flux (PDF), and precision is illustrated by the degree of agreement in flux estimates. The following scenarios are illustrated: (A) high bias/low precision, (B) high bias/high precision, (C) low bias/low precision, and (D) low bias/high precision (the ideal outcome).

recommend any single, uniform approach with regard to chamber geometry, deployment time, or flux calculation that will be optimal across all measurement conditions. However, based on our current understanding, the following practices and considerations relative to chamber-induced biases are recommended:

1. In cases where soil property effects would be expected to confound data interpretation (as discussed above), or in cases where estimates of the *absolute* flux magnitude is of primary importance, measures described above to evaluate the degree of bias (e.g. using the CEAT method, especially when initially designing chambers) or correct for bias (e.g. using the CBC method) should be considered. Due to natural variation in soil water content, this will include many if not the vast majority of situations.
2. While many chamber versus time data sets appear to be highly linear, gas transport theory has shown that even data displaying  $r^2$  values greater than 0.99 can result in substantial flux underestimation using LR. Thus, while it is tempting to apply LR, it is not recommended as a primary method unless combined with bias correction techniques. Several researchers have used the approach of making preliminary or periodic evaluations of linearity to justify using LR and also to justify using a reduced number of sampling points based on the assumption of linearity. However, because soil conditions (e.g. water content) can directly affect the degree of linearity, this approach is also not recommended. Thus, non-linear FC schemes are recommended, using four time points at a minimum.
3. While we cannot at this time recommend any one specific FC scheme, analysis to date indicates that the quadratic FC scheme (Wagner et al., 1997) generates flux estimates with lower bias than LR but greater precision than the HM method, when both the quadratic and HM schemes are applied with a reasonable model failure criteria (Venterea et al., 2009). Thus, an argument can be made that the quadratic method best balances the bias and precision trade-off. An additional benefit is that the quadratic method does not require equally spaced time points. Preliminary analysis has indicated that selection of the optimal FC scheme based on the mean square error (which incorporates both bias and precision) may vary depending on measurement conditions (i.e.  $H$ ,  $DP$ , soil properties) (Parkin and

Venterea, 2010). Ongoing analysis is evaluating the benefits of the newly developed HMR scheme, which also does not require equally spaced time points (Parkin et al., unpublished data).

4. The precision of the sampling and analytical method used to determine chamber gas concentrations should be quantified by making repeated (i.e.  $\geq 20$ ) measurements of samples of standard gases that are collected and analyzed as similarly as possible to actual chamber samples. The sampling and analytical precision can then be used to determine (1) the overall precision of the flux estimate accounting for DP,  $H$ , and soil properties, using the method of Venterea et al. (2009), and (2) the minimum detectable flux using the methods of Parkin et al. (2012).

In addition to the above recommendations, the reader is also directed to Parkin and Venterea (2010) and Hutchinson and Livingston (2002).

## ULTIMATE SOLUTIONS

The bias-precision trade-off problem would disappear if sampling and analytical error were eliminated, in which case very short DPs and large  $H$  values together with Type II non-linear FC schemes could largely eliminate chamber-induced bias. While it is not realistic to expect complete error elimination, advances in measurement instrumentation have the potential to greatly reduce errors. Relatively low-cost instrumentation is available that can measure near-ambient CO<sub>2</sub> concentrations with relatively high precision. That is, real-time infrared analyzers can be used in conjunction with NSS chambers to make flux estimates using DPs less than 5 min which can largely eliminate chamber-induced biases with acceptable precision (e.g. Davidson et al., 2002). While high-precision, high-sensitivity analyzers for use with N<sub>2</sub>O flux measurements have been introduced and have potential to achieve the same result (e.g. Laville et al., 2011), the reliability of some of these analyzers has been questioned (e.g. Flechard et al., 2007; Yamulki and Jarvis, 1999) and will require further testing. Also, high-precision analyzers generally require real-time, in-situ analysis, in contrast with more commonly used techniques such as gas chromatography which require collection of discrete gas samples for subsequent analysis. While real-time analysis has its advantages, it also has limitations in that only one chamber location can be measured at one time per analyzer in contrast with discrete sample collection techniques which can utilize rotational sampling regimes to sample multiple locations at one time. Use of high-precision N<sub>2</sub>O analyzers in combination with automated chamber technology could partly overcome this limitation although the degree of replication that is practical with automated chambers is generally less than can be achieved with manual chambers. While micrometeorological methods for N<sub>2</sub>O flux determination avoid chamber-related issues altogether, they have their own set of limitations (Hutchinson and Livingston, 2002). In addition, the practical utility of micrometeorological methods for use in replication plot studies aimed at detecting statistically significant treatment effects is limited.

## References

- Butnor, J.R., Johnsen, K.H., 2004. Calibrating soil respiration measures with a dynamic flux apparatus using artificial soil media of varying porosity. *Eur. J. Soil Sci.* 55, 639–647.
- Butnor, J.R., Johnsen, K.H., Maier, C.A., 2005. Soil properties influence estimates of soil CO<sub>2</sub> efflux from three chamber-based measurement systems. *Biogeochemistry* 73, 283–301.
- Chapuis-Lardy, L., Wrage, N., Metay, A.L., Chotte, J., Bernoux, M., 2007. Soils, a sink for N<sub>2</sub>O? A review. *Global Change Biol.* 13, 1–17.
- Davidson, E.A., Savage, K., Verchot, L.V., Navarro, R., 2002. Minimizing artifacts and biases in chamber-based measurements of soil respiration. *Agr. Forest Meteorol.* 113, 21–37.
- Flechard, C., Ambus, P., Skiba, U., Rees, R., Hensen, A., van Amstel, A., et al., 2007. Effects of climate and management intensity on nitrous oxide emissions in grassland systems across Europe. *Agricult. Ecosys. Environ.* 121, 135–152.

- Fuller, E.N., Schettler, P.D., Giddings, J.C., 1966. A new method for prediction of binary gas-phase diffusion coefficients. *Ind. Eng. Chem.* 58, 19–27.
- Griffiths, E., 1926. *Methods of Measuring Temperature*, second ed. Charles Griffin and Co, London, p. 203.
- Healy, R.W., Striegl, R.G., Russell, T.F., Hutchinson, G.L., Livingston, G.P., 1996. Numerical evaluation of static-chamber measurements of soil–atmosphere gas exchange: identification of physical processes. *Soil Sci. Soc. Am. J.* 60, 740–747.
- Hutchinson, G.L., Livingston, G.P., Healy, R.W., Striegl, R.G., 2000. Chamber measurement of surface-atmosphere trace gas exchange: numerical evaluation of dependence on soil, interfacial layer, and source/sink properties. *J. Geophys. Res. Atm.* 105 (D7), 8865–8875.
- Hutchinson, G.L., Mosier, A.R., 1981. Improved soil cover method for field measurement of nitrous oxide fluxes. *Soil Sci. Soc. of Am. J.* 45, 311–316.
- Hutchinson, G.L., Livingston, G.P., 2001. Vents and seals in nonsteady-state chambers used for measuring gas exchange between soil and the atmosphere. *Eur. J. Soil Sci.* 52, 675–682.
- Hutchinson, G.L., Livingston, G.P., 2002. Soil-atmosphere gas exchange. In: Dane, J.H., Topp, G.C. (Eds.), *Methods of Soil Analysis. Part 4. SSSA Book Ser. 5. SSSA, Madison, WI*, pp. 1159–1182.
- Hutchinson, G.L., Rochette, P., 2003. Non-flow-through steady-state chambers for measuring soil respiration: numerical evaluation of their performance. *Soil Sci. Soc. Am. J.* 67, 166–180.
- Kroon, P.S., Hensen, A., van den Bulk, W.C.M., Jongejan, P.A.C., Vermeulen, A.T., 2008. The importance of reducing the systematic error due to non-linearity in N<sub>2</sub>O flux measurements by static chambers. *Nutrient Cycl. Agroecosys* 82, 175–186.
- Kutzbach, L., Schneider, J., Sachs, T., Giebels, M., Nykänen, H., Shurpali, N.J., Martikainen, P.J., Alm, J., Wilmking, M., 2007. CO<sub>2</sub> flux determination by closed-chamber methods can be seriously biased by inappropriate application of linear regression. *Biogeosci. Disc.* 4, 2279–2328.
- Laville, P., Lehuger, S., Loubet, B., Chaumartin, F., Cellier, P., 2011. Effect of management, climate and soil conditions on N<sub>2</sub>O and NO emissions from an arable crop rotation using high temporal resolution measurements. *Agr. Forest Meteorol* 151, 228–240.
- Livingston, G.P., Hutchinson, G.L., Spartalian, K., 2006. Trace gas emission in chambers: a non-steady-state diffusion model. *Soil Sci. Soc. Am. J.* 70, 1459–1469.
- Martin, J.G., Bolstad, P.V., Norman, J.M., 2004. A carbon dioxide flux generator for testing infrared gas analyzer-based soil respiration systems. *Soil Sci. Soc. Am. J.* 68, 514–518.
- Matthias, A.D., Yarger, D.N., Weinback, R.S., 1978. A numerical evaluation of chamber methods for determining gas fluxes. *Geophys. Res. Lett.* 5, 765–768.
- Ney, M.S., Mattson, K.G., Bormann, B.T., 1994. Biases of chamber methods for measuring soil CO<sub>2</sub> efflux demonstrated with a laboratory apparatus. *Ecology* 75, 2460–2463.
- Omonode, R.A., Smith, D.R., Gál, A., Vyn, T.J., 2011. Soil nitrous oxide emissions in corn following three decades of tillage and rotation treatments. *Soil Sci. Soc. Am. J.* 75, 152–163.
- Parkin, T.B., Venterea, R.T., 2010. USDA-ARS GRACEnet Project Protocols. Chapter 3. Chamber-Based Trace Gas Flux Measurements (replaces 2003 version). Available at <http://www.ars.usda.gov/SP2UserFiles/Program/212/Chapter%203.%20GRACEnet%20Trace%20Gas%20Sampling%20Protocols.pdf>.
- Parkin, T.B., Venterea, R.T., Hargreaves, S.K., 2012. Calculating the detection limits of chamber-based soil greenhouse gas flux measurements. *J. Environ. Qual.* (In press).
- Pedersen, A.R., Petersen, S.O., Schelde, K., 2010. A comprehensive approach to soil atmosphere trace-gas flux estimation with static chambers. *Eur. J. Soil Sci.* 61, 888–902.
- Pumpanen, J., Kolari, P., Ilvesniemi, H., Minkkinen, K., Vesala, T., Niinistö, S., Lohila, A., et al., 2004. Comparison of different chamber techniques for measuring soil CO<sub>2</sub> efflux. *Agricult. For. Meteorol* 123, 159–176.
- Rochette, P., Eriksen-Hamel, N.S., 2008. Chamber measurements of soil nitrous oxide flux: are absolute values reliable? *Soil Sci. Soc. Am. J.* 72, 331–342.
- Rochette, P., Angers, D.A., Chantigny, M.H., Gagnon, B., Bertrand, N., 2008. N<sub>2</sub>O fluxes in soils of contrasting textures fertilized with liquid and solid dairy cattle manures. *Can. J. Soil Sci.* 88, 175–187.
- Rolston, D.E., Moldrup, P., 2002. Gas diffusivity. In: Dane, J.H., Topp, G.C. (Eds.), *Methods of Soil Analysis. Part 4. SSSA Book Ser. 5. SSSA, Madison, WI*, pp. 1113–1139.
- Sander, R., 1999. *Compilation of Henry's Law Constants for Inorganic and Organic Species of Potential Importance in Environmental Chemistry (Version 3)*. <http://www.henrys-law.org> (confirmed August 27, 2009).
- Senevirathna, D.G.M., Achari, G., Hettiaratchi, J.P.A., 2007. A mathematical model to estimate errors associated with closed flux chambers. *Environ. Model. Assess.* 12, 1–11.
- Snoeyink, V.L., Jenkins, D., 1980. *Water Chemistry*. John Wiley & Sons, New York.
- Venterea, R.T., 2010. Simplified method for quantifying theoretical underestimation of chamber-based trace gas fluxes. *J. Environ. Qual.* 39, 126–135.

- Venterea, R.T., Baker, J.M., 2008. Effects of soil physical nonuniformity on chamber-based gas flux estimates. *Soil Sci. Soc. Am. J.* 72, 1410–1417.
- Venterea, R.T., Spokas, K.A., Baker, J.M., 2009. Accuracy and precision analysis of chamber-based nitrous oxide gas flux estimates. *Soil Sci. Soc. Am. J.* 73, 1087–1093.
- Wagner, S.W., Reicosky, D.C., Alessi, R.S., 1997. Regression models for calculating gas fluxes measured with a closed chamber. *Agron. J.* 89, 279–284.
- Widen, B., Lindroth, A., 2003. A calibration system for soil carbon dioxide-efflux measurement chambers: description and application. *Soil Sci. Soc. Am. J.* 67, 327–334.
- Yamulki, S., Jarvis, S.C., 1999. Automated chamber technique for gaseous flux measurements: evaluation of a photoacoustic infrared spectrometer trace gas analyzer. *J. Geophys. Res.* 104, 5463–5469.

## APPENDIX: STEPS AND CALCULATIONS USED IN CBC METHOD

**Note:** A spreadsheet that can be used as a template for the calculations given below is available for downloading at <http://www.ars.usda.gov/pandp/people/people.htm?personid=31831> or upon request from the authors.

**Note about units:** The required parameter inputs with units and symbols are listed in Table A1. Units selected for the soil input parameters need to be consistent with the units used for  $H$  and  $DP$ . For example, in Table A1, all  $L$  units are in cm and  $T$  units are in h. Thus<sup>b</sup>,  $h$  must be used as the time unit for  $DP$  and cm as the length unit for  $H$ . This will result in a dimensionless term inside the parentheses and for  $E_2$  in Eq. [A8]. Any set of units can be used to calculate the initial uncorrected flux estimate ( $F$ ), i.e. units for  $F$  do not have to be consistent with units for  $E_1$ ,  $H$ , or  $DP$ , and the corrected PDF will always have the same units as  $F$ .

**Note about high-organic or high-clay soils:** For soils with clay content >40% or organic matter >5%, Eq. [A7] may need to be modified for greater accuracy. For these cases, the reader is referred to the theory section of Venterea (2010).

Steps for using the chamber-bias correction technique of Venterea (2010):

1. Calculate  $F$  in the conventional manner using either linear regression, the Type I quadratic method of Wagner et al. (1997), or the Type II method of Hutchinson and Mosier (1981) together with Eq. [1].
- 2a. Calculate the following intermediate parameters needed for determining  $E_1$ :  
Volumetric water content ( $\theta$ ) (if only gravimetric water content  $\theta_g$  is known):

$$\theta = \theta_g \rho \quad [A1]$$

Total porosity ( $\phi$ ):

$$\phi = \left( 1 - \frac{\rho}{\rho_p} \right) \quad [A2]$$

Henry's law gas–liquid partitioning coefficient ( $K$ ):

$$K = K_{25} \exp \left[ \chi \left( \frac{1}{T_s + 273.15} - \frac{1}{298.15} \right) \right] \quad [A3]$$

where  $K_{25}$  is the Henry's constant at 25°C, and  $\chi$  is a temperature response factor (Sander, 1999). Values for  $K_{25}$  and  $\chi$  are listed in Table A1.

<sup>b</sup> More rigorously, the actual units of  $H$  are not cm but really  $\text{cm}^3 \text{ gas cm}^{-2} \text{ soil}$ . Thus, the actual units of  $E_1$  in the examples are  $\text{cm}^6 \text{ gas cm}^{-4} \text{ soil h}^{-1}$  (Table 19.2).

**TABLE A1** Parameter Values for use in Eqs. [A3] and [A4]

	$K_{25}^{\dagger}$	$K^{\ddagger}$	$D_{25}^{\ddagger}$
Gas	$\text{cm}^3 \text{ gas cm}^{-3} \text{ H}_2\text{O}$	K	$\text{cm}^2 \text{ h}^{-1}$
$\text{N}_2\text{O}$	0.6116	2600	511.7
$\text{CO}_2$	0.8318	2400	652.3

<sup>†</sup>Sander (1999).

<sup>‡</sup>Fuller et al. (1966); Healy et al. (1996).

Gas diffusivity in free air (D):

$$D = D_{25} \left[ \frac{273.15 + T_s}{298.15} \right]^{1.72} \quad [\text{A4}]$$

where  $D_{25}$  is the diffusivity at 25°C (Rolston and Moldrup, 2002). Values for  $D_{25}$  are listed in Table A1.

Campbell soil pore-size distribution parameter (b):

$$b = 13.6 \text{ CF} + 3.5 \quad [\text{A5}]$$

where  $CF$  is the clay fraction ( $0 < CF < 1$ ) (Rolston and Moldrup, 2002).

Correction factor for pH (applicable to  $\text{CO}_2$  only) ( $\beta$ ):

$$\beta = 1 + 10^{(\text{pH} - \text{p}K_a)} + 10^{(2\text{pH} - \text{p}K_a - \text{p}K_b)} \quad [\text{A6}]$$

where  $\text{p}K_a = 6.42$  and  $\text{p}K_b = 10.43$  are the equilibrium constants for dissociation of carbonic acid and bicarbonate, respectively (values at 25°C per Snoeyink and Jenkins, 1980). If desired, values of  $\text{p}K_a$  and  $\text{p}K_b$  at varying temperature can be found in Table 4-7 of Snoeyink and Jenkins (1980). The  $\beta$  parameter accounts for the formation of soluble carbonate species from dissolved  $\text{CO}_2$  which will also influence chamber  $\text{CO}_2$  dynamics (Hutchinson and Rochette, 2003). Since pH is not expected to affect  $\text{N}_2\text{O}$  gas-liquid partitioning,  $\beta$  should be set equal to 1 for  $\text{N}_2\text{O}$ . For  $\text{CO}_2$ ,  $\beta$  reduces to 1 for pH less than approximately 5.0.

**2b.** Once the above intermediate terms are calculated,  $E_1$  can be calculated from

$$E_1 = [\varphi + \theta(\beta K - 1)] D \varphi^2 (1 - \theta/\varphi)^{(2+3/b)} \quad [\text{A7}]$$

**2c.**  $E_2$  is then calculated from

$$E_2 = \ln \left( \frac{H^2}{E_1 DP} \right) \quad [\text{A8}]$$

**TABLE A2** Regression Coefficients Required for Calculating the Theoretical Flux Underestimation (TFU) in Eq. [A9] for Different Flux-Calculation Schemes

Flux-calculation scheme	Regression coefficient			
	$a$	$b$	$c$	$d$
LR	44.3456	-5.5105	0.1799	0.0363
HM <sup>†</sup>	25.0140	-3.2561	0.2772	0.0439
Quadratic <sup>‡</sup>	26.8575	-3.5666	0.2814	0.0471

<sup>†</sup>Model of Hutchinson and Mosier (1981).

<sup>‡</sup>Model of Wagner et al. (1997).



**2d.** TFU is then determined from

$$TFU = \frac{a + bE_2}{1 + cE_2 + dE_2^2} \quad [A9]$$

where  $E_2$  is dimensionless,  $TFU$  is expressed as a percentage, and  $a$ ,  $b$ ,  $c$ , and  $d$  are regression coefficients specific to each FC scheme, as shown in Table A2.

**3.** And finally, the PDF is determined from

$$PDF = \frac{F}{\left(1 - \frac{TFU}{100}\right)} \quad [A10]$$

where PDF has the same units as  $F$ .

